

PRESSURE EVALUATION AT ARBITRARY LOCATIONS IN SPH WATER IMPACT SIMULATIONS

MARTIN SIEMANN¹ AND PAUL GROENENBOOM²

¹ German Aerospace Center
Pfaffenwaldring 38-40
70569 Stuttgart, Germany
Martin.Siemann@dlr.de – <http://www.dlr.de>

² ESI Group Netherlands
Rotterdamseweg 183 C
2629 HD Delft, The Netherlands
pgr@esi-group.com – <http://www.esi-group.com>

Key words: Smoothed Particle Hydrodynamics, Fluid-Structure Interaction, Pressure evaluation, Fixed-Wing Aircraft Ditching, Hydrodynamic Phenomena

Abstract. This paper reports the application of the SPH method to the simulation of structures impacting on water with the focus on pressure assessment at arbitrary positions. The study is motivated by the importance of correct and reliable pressure evaluation in aircraft ditching simulations. The presented approach refers to recent developments in the SPH solver of VPS/PAM-CRASH which now allows using dummy particles to probe pressures. Sensitivity studies towards SPH parameters on pressure results are conducted. Pressures near contact interfaces are also compared to the local contact force divided by the surface area. Furthermore, pressure correction methods referred to as Shepard filtering and Rusanov flux, the lowest order approximation of a Riemann solver, are applied and tested. A comparison with results from flat plate ditching experiments published by Smiley [1] is done. Initial validation is based upon results of an experimental campaign of rigid wedge impacts conducted by Battley et al. [2]. Recommendations for best practice are derived from the study and the application to aircraft ditching is discussed.

1 INTRODUCTION

The prediction of global and local structural loads is of fundamental importance in water impact problems, e. g. aircraft ditching. These loads significantly differ from those in a crash on solid ground [3]. One key value affecting the structural response is the pressure acting along the structure. It may affect the global kinematic response of an aircraft, therefore leading to catastrophic failure of the aircraft accompanied by fatalities.

Ditching refers to an aircraft emergency situation which ends with the planned impact on water. A ditching event is typically described in four consecutive phases: approach, impact, landing and floatation. However, the present work considers exclusively the impact phase (figure 1). The presence of a relatively high forward velocity in fixed-wing aircraft ditching affects the pressure distribution and the interrelated hydrodynamic effects acting on the fuselage. Consequently, the pressure distribution highly influences structural loads and, as a result, the global aircraft kinematics which may determine the survivability of such an emergency situation. The analysis of ditching impact is therefore necessary to satisfy the airworthiness regulations in certification of novel aircraft. Readers are referred to publications of Toso [3], Benítez et al. [4], Climent et al. [5], and Lindenau et al. [6] for a more detailed view on all ditching phases.

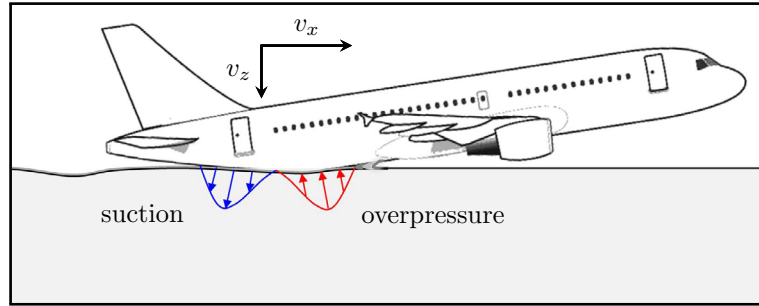


Figure 1: Impact phase of fixed-wing aircraft ditching with emphasis on the pressure distribution along the rear fuselage due to hydrodynamic phenomena, e. g. cavitation, ventilation, overpressure, suction, air entrapment, and air cushioning.

In the present work, pressure assessment at arbitrary locations along moving structures is studied using coupled SPH-FE simulation models. Attention is put on improving the well-known discrepancy of numerical noise in SPH pressure results. Results of this work aim to allow studying the above mentioned hydrodynamic phenomena in more detail. This may contribute to the development of improved fluid and fluid-structure interaction models for aircraft ditching analysis as currently these are not satisfactory mastered by existing simulation tools.

2 FLUID-STRUCTURE INTERACTION: COUPLED SPH-FE MODELS

The presented numerical simulations are based on fully coupled SPH and explicit FE simulation models which—among the variety of numerical simulation tools used to assess fluid-structure interaction—offer a convenient analysis tool. The commercial explicit Finite Element software VPS/PAM-CRASH (ESI Group) with Lagrangian formulation is used.

The **structural models** are composed of rigid FE shell elements. Their movement is prescribed by an initial velocity vector and it is constrained by limiting the degrees of freedom to model the guidance of the structure according to the respective experiments.

The **fluid domain** is modeled using the weakly compressible SPH method. Particles are initially arranged on a cubic lattice configuration with particle spacing s (orthogonally spaced) and are bounded in a box of rigid shell elements or hydrodynamic solid elements. The free surface does not necessitate boundary conditions. For two-dimensional cases, in-plane displacement is constrained. The Wendland kernel function (5th degree class 2) with a radius of influence of twice the smoothing length h is applied. This kernel function was shown to be superior over the renormalized Gaussian kernel in free-surface flow problems by Macià et al. [7]. The numerical stability is treated by using the standard Monaghan-Gingold artificial viscosity term [8]. The constitutive equation (1) relating fluid density ρ to pressure p refers to the Murnaghan (Tait) equation of state. It defines the pressure $p(\rho)$ as

$$p(\rho) = p_0 + \underbrace{\frac{c_0^2 \rho_0}{\gamma}}_B \left[\left(\frac{\rho}{\rho_0} \right)^\gamma - 1 \right] \quad (1)$$

wherein p_0 is the reference pressure, c_0 is the speed of sound in the fluid at the state $\rho = \rho_0$, B is the bulk modulus, ρ/ρ_0 is the ratio of current over initial mass density and γ is the adiabatic exponent of the fluid. The Murnaghan equation of state allows representing a fluid with artificially increased compressibility. This approach is feasible for fluid-structure interaction problems where flow velocities \mathbf{u} remain well below the corresponding speed of sound and hence compressibility effects are insignificant [9, 10]. Satisfying the equation $c_0 \geq 10 \max(\mathbf{u})$, this criteria may be expressed as

$$B \geq 100 \frac{\rho_0 \max(\mathbf{u})^2}{\gamma} . \quad (2)$$

Assuming typical aircraft ditching conditions, the flow velocities are much lower than the true speed of sound in water. This condition allows using a reduced speed of sound which (automatically) increases the critical time step of the SPH particles (governing the simulation's critical time step) and, hence, decreases the run time of the simulation. For the studies in this work, the bulk modulus is chosen depending on the corresponding maximum flow velocity in the regarded test cases. As compressibility is essential for impact phenomena, the influence of the bulk modulus on pressure results was verified and found to be negligible within the investigated range of maximum flow velocities.

Coupling the SPH and the FE model is achieved by using a node-to-segment penalty contact formulation between the particles and the impacting FE structure. Contrary to results published by Aquelet and Souli [11], within this work, contact damping (stiffness proportional) was found to not influence the numerical noise in pressure results. Further information regarding the penalty contact algorithm of VPS/PAM-CRASH may be found in [12].

3 SPH PRESSURE CORRECTION METHODS

The standard weakly compressible SPH method is well known to give poor pressure distributions in terms of high-frequency oscillations (numerical noise) in time and space. This deficiency is counteracted by pressure correction methods which aim to yield a more regular pressure distribution. However, the effect of correction should be local and not smooth global flow characteristics. Conservation of mass, momentum, and energy should be maintained or changes in the conservation should remain very small. Furthermore, correction methods must be numerically stable and may not require considerably higher amounts of computational power.

Established pressure correction methods like density re-initialization by Shepard filtering and Rusanov flux were recently implemented in the SPH solver of VPS/PAM-CRASH. In this section, the fundamentals of the respective correction methods are presented and their superiority on pressure results is demonstrated in figure 2.

3.1 Density Re-Initialization using Shepard Filtering

One method which may reduce numerical noise in SPH pressure field computation is referred to as the Shepard filter. This density re-initialization method was derived from an interpolation technique initially published by Shepard [13]. As the SPH pressure calculation is based on an equation of state including the fluid density, re-initializing the density by Shepard filtering directly influences the pressure distribution. The implemented SPH notation for the modified density $\tilde{\rho}_i$ reads

$$\tilde{\rho}_i = \sum_j^N m_j \frac{W_{ij}}{\sum_k^N \frac{m_k}{\rho_k} W_{jk}} \quad (3)$$

where m_j and ρ_j are mass and respective mass density of particle j and W_{ij} is the kernel function.

The density field is periodically re-initialized at a user-defined cycle frequency f with recommended values of 20 [14]. In general, numerical noise originating from the weakly compressible SPH solution may be reduced and the pressure field therefore may become much smoother. The additional computational cost of this correction method is negligible.

3.2 Rusanov Flux: A Non-Conservative Riemann Solution

The Rusanov flux is an efficient and robust, but also more diffusive, numerical scheme to solve Riemann problems. This approximation of a Riemann solver achieves only first order accuracy compared to second order accuracy of the Riemann flux. The used formulation was proposed by Parshikov et al. [15,16] and later by Cha and Whitworth [17] as Godunov Particle Hydrodynamics (GPH). In 1D, the continuity equation is modified to

$$\frac{d\rho}{dt} = -2 \sum_j^N m_j (u_{ij}^* - u_i) \nabla_i W_{ij} \quad (4)$$

in which the intermediate velocity u_{ij}^* is the acoustic solution (5).

$$u_{ij}^* = \frac{\rho_i c_i u_j^R + \rho_j c_j u_i^R + P_i - P_j}{\rho_i c_i + \rho_j c_j} \quad (5)$$

Assuming that variations in density and sound speed remain small, and that the time step obeys the Courant criterion, the continuity equation becomes

$$\frac{\rho^{n+1} - \rho^n}{\Delta t} = \sum_j^N m_j (\mathbf{u}_i^n - \mathbf{u}_j^n) \cdot \nabla_i W_{ij} - 2\epsilon \sum_j^N \frac{m_j}{\rho_j} \frac{(P_i^n - P_j^n) \mathbf{r}_{ij} \cdot \nabla_i W_{ij}}{(r_{ij}^2 + \chi h^2)} \Delta t \quad (6)$$

with the strength parameter ϵ in the order of one-half [23]. Further, the solution of the acoustic approximation for the velocities adds an expression similar to the regular artificial viscosity in the momentum equation.

As previously shown by Groenenboom [23], this correction method does not significantly influence forces and kinematics of the impacting structure. The additional computational cost is negligible while in practice run times decrease slightly due to reduced numerical noise in the density field.

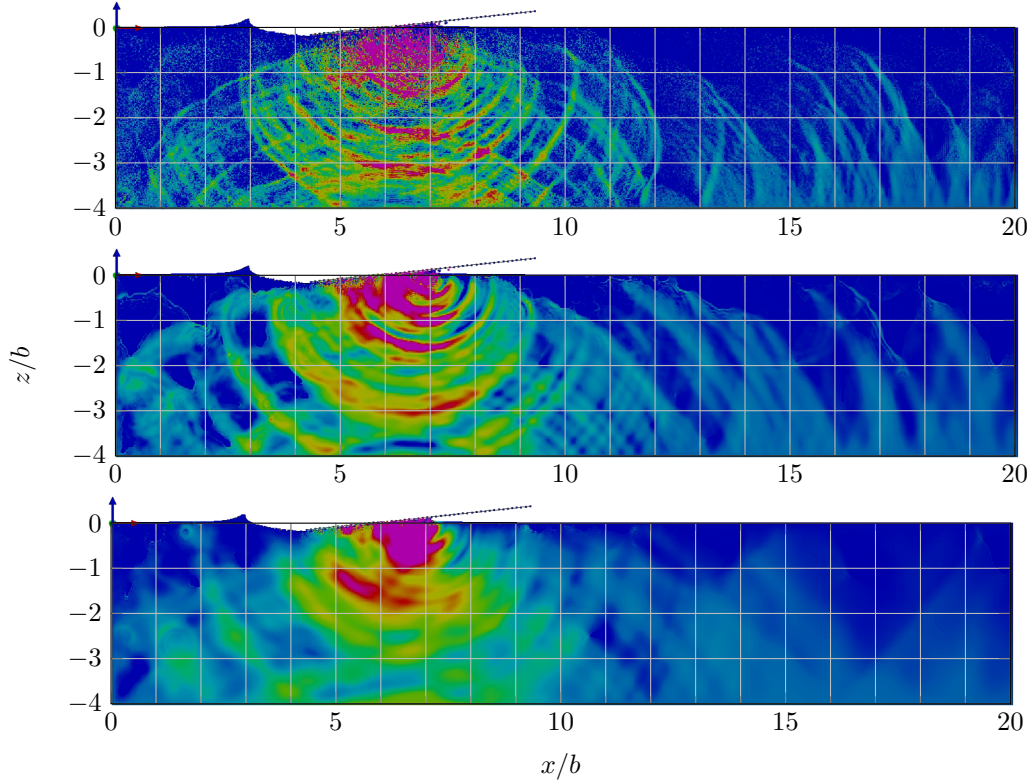


Figure 2: Pressure field at $t = 30 \text{ ms}$ in 2D NACA flat plate test case using no correction (top), Shepard filtering with cycle frequency $f = 20$ (center), and Rusanov flux with strength $\epsilon = 0.5$ (bottom).

4 PRESSURE EVALUATION METHODS

4.1 SPH Pressure Gauge Particles

VPS/PAM-CRASH now allows using dummy SPH particles to probe pressures. Main advantages are that pressure information may be obtained at any desired location (fixed or moving in space) and, since the pressure is averaged over a number of nearby particles, it will suffer less from the strong spatial fluctuations typical for SPH pressures. Pressure gauge particles are defined as a special type of particle and may be described as passive particles which probe the properties of nearby regular particles but do not contribute to the evaluation of their SPH properties. To facilitate pressure assessment, gauge particles may be attached to moving structures or be put at arbitrary locations. Refer to figure 3 for a detailed view.

The gauge smoothing length h_g is the main numerical parameter to be investigated and calibrated. It determines the amount of regular particles contributing to the pressure evaluation of the gauge and will clearly influence the stability in case of rather small values. Furthermore, it is expected that pressures assessed with gauge particles will be subject to smoothing in case the gauge smoothing length is chosen too large. In order to generalize findings, the gauge smoothing length is chosen proportional to that of the regular particles which is defined as gauge size ratio $\Pi = h_g/h$.

4.2 Pressure via Contact Normal Force over Contact Area

Another, to date frequently used method assessing pressures in numerical simulations is given by calculating the contact normal force over contact area. Here, pressure time histories depend on the ratio of regular particles per shell element and, furthermore, on the size of the contact area A_{cont} . The latter may cause averaging over too many shell elements (too large area) which may smear out pressure peaks (local information) from the pressure time history. Figure 3 provides a schematic illustration.

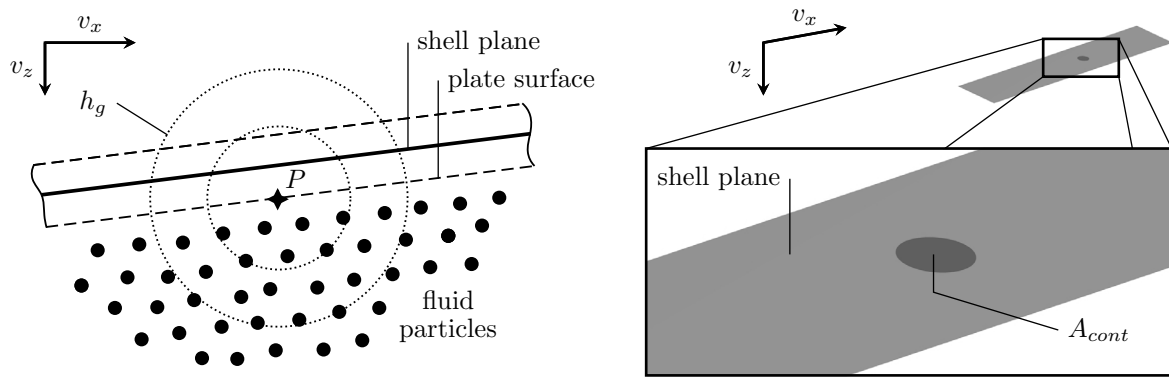


Figure 3: Detailed view on pressure evaluation methods: 2D view showing position and size of gauge particle P (left), and pressure assessment via contact normal force over contact area in 3D cases (right).

5 TEST CASES

5.1 Two-Dimensional Rigid Wedge Vertical Impact

This first test case was taken from Battley et al. [2], who performed motion-controlled vertical impact experiments using a rigid wedge of 10° deadrise angle impacting with constant velocity of 3 m/s (servo-hydraulic controlled). Experimental pressure results are available for three positions along the center line between keel and chine which has a total length of 600 mm . Further information about the instrumentation, the data acquisition, and the servo-hydraulic slam testing system may be found in [2].

The numerical model is symmetrical with respect to the vertical axis. It consists of a wedge structural model and a two-dimensional water domain filled with particles with smoothing length of $h = 2\text{ mm}$. Pressure gauge particles with a smoothing length of $h_g = 4\text{ mm}$ ($\Pi = 2$) are positioned on the actual surface location of the wedge.

Numerical pressure results using the previously described pressure gauge particles are validated against experimental data in figure 4. Numerical pressure time histories are CFC1000-filtered. Comparison between experimental and numerical pressure time histories shows good correlation of peak values. However, after peaks diminish, the numerical residual pressures are higher compared to the experimental ones. It is believed that the general overestimation of pressures in the simulation is caused by the two-dimensional nature of the numerical model. Nevertheless, it has been demonstrated that the pressure gauge particles allow for reasonable pressure results for this test case.

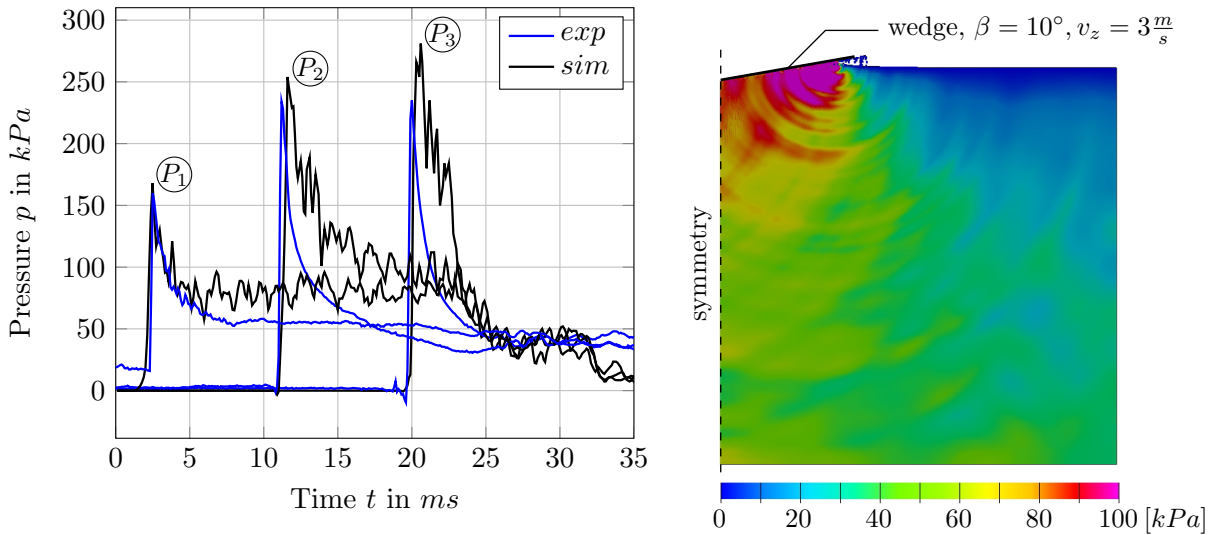


Figure 4: Comparison of experimental and numerical pressure results: Time histories at positions P_1 – P_3 and pressure contour plot at $t = 20\text{ ms}$.

5.2 Two-Dimensional NACA Flat Plate Ditching

Due to lack of experimental data to validate the novel pressure assessment method using gauge particles under ditching conditions, flat plate ditching experiments published by Smiley [1] in 1951 are selected as a test case for this numerical parameter study. Nevertheless, initial velocities are smaller compared to fixed-wing aircraft ditching characteristics.

The selected test configuration (run 4 in [1]) consists of a flat plate ($1524\text{ mm} \times 304.8\text{ mm} \times 18.288\text{ mm}$, pitch angle $\alpha = 6^\circ$), which is connected to a trolley moving along a guidance structure during the entire experiment with a prescribed motion in terms of initial velocities in horizontal and vertical direction ($v_x = 13.35\text{ m/s}$ and $v_z = 1.77\text{ m/s}$). 18 flush mounted pressure gauges with 12.70 mm diameter and one bellow-type pressure gauge with 6.35 mm diameter were used. Data was acquired at a rate of 1 kHz . However, only eleven time instances are available for the selected case. As this is insufficient for a comparison of pressure time histories, the parameter study compares numerical pressure results to experimental maximum pressures along the center line which vary between 300 kPa and 400 kPa . One pressure gauge measured a higher maximum pressure of 427 kPa which is believed to be related to its smaller size (diameter 6.35 mm).

The numerical model consists of a flat plate structural model and a two-dimensional water domain (see figure 2). Multiple pressure gauge particles are attached to the structure at the actual surface location of the plate. Within an extensive parameter study, gauge size ratios ranging between $\Pi = 1 - 10$ were investigated using different global finesse of $b/s = 10 - 100$ which refers to the particle spacing s normalized on the width b of the plate. Below results refer to a particle spacing of $s = 6.1\text{ mm}$ (corresponding to $b/s = 50$) which gives reasonable results. Pressure data are compared at $\xi = 0.4$ ($\xi \in [0, 1]$ is the relative local plate coordinate in longitudinal direction measured from the trailing edge).

Numerical pressure results assessed by pressure gauge particles are compared to maximum pressures from the respective experiments. Similar to observations in the experiments, numerical results show a sharp and immediate rise of the pressure during impact. The pressure peak travels with the ditching front along the plate until its full submersion where pressures become significantly lower. Pressure results of this study are analyzed in figure 5. Regarded pressure correction methods influence the oscillations which are smallest when using the Rusanov flux. Filtering of pressure signals is a critical issue as it may significantly alter peak pressure values. Hence the influence of filtering was studied for different gauge size ratios revealing that filtering reduces pressure peak values especially for ratios below $\Pi = 3$. Furthermore, there is a significant influence of the gauge size ratio on the pressure time histories. With increasing gauge size ratio, pressure peaks as well as pressure gradients and associated oscillations are reduced (smoothing effect), but the later residual pressures remain at similar level of magnitude. Based on the presented study, it is recommended to chose the gauge size ratio as small as possible but no less than $\Pi = 2$.

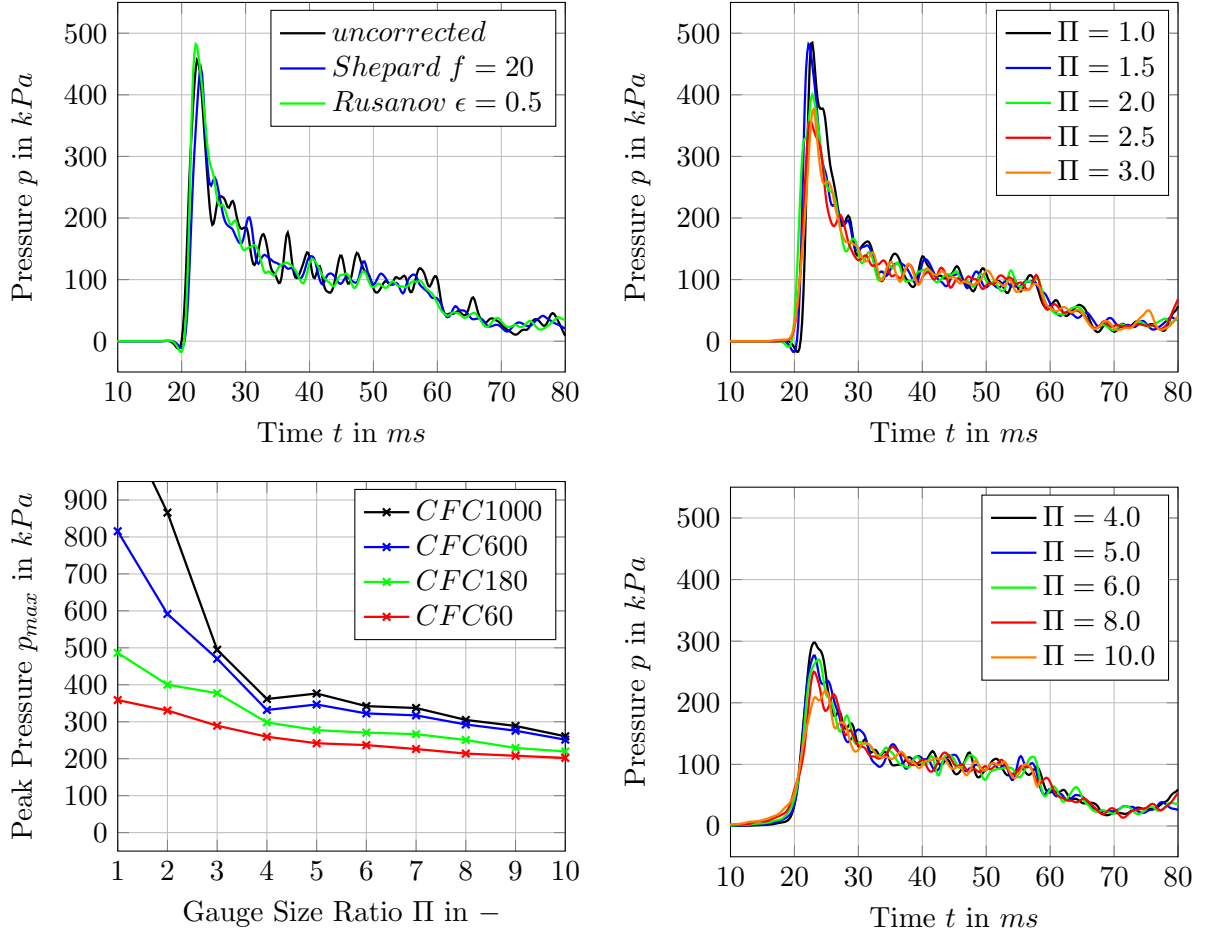


Figure 5: Numerical pressure time histories at position $\xi = 0.4$ comparing the influence of pressure correction methods (top left), gauge size ratio Π (top and bottom right), and filtering (bottom left).

5.3 Three-Dimensional Guided Ditching Test

The novel pressure assessment method using gauge particles was applied to the three-dimensional numerical model of the guided ditching tests to be carried out within the EC-funded research project SMAES (SMart Aircraft in Emergency Situations) [4, 18–20]. The guided ditching simulation model is shown on the right hand side of figure 6. For the selected load case, the initial velocities are $v_x = 50.0 \text{ m/s}$ in horizontal and $v_z = 1.5 \text{ m/s}$ in vertical direction. The flat plate measures $1000 \text{ mm} \times 500 \text{ mm} \times 15 \text{ mm}$ and is assumed to be rigid. Throughout the simulation, the pitch angle of 10° remains constant due to the guided motion. Fluid particles have a smoothing length of $h = 10 \text{ mm}$ and gauge particles of $h_g = 20 \text{ mm}$ ($\Pi = 2$) respectively. The contact surface used for the pressure evaluation has an area of $A_{cont} = 1600 \text{ mm}^2$. Results are compared at the position $\eta = 0$ (center line regarding the lateral direction) and $\xi = 0.25$.

Pressure results presented in figure 6 show a good qualitative correlation between the signals obtained by the two different pressure assessment methods (p_{cont} and p_{gauge}). There is a time shift of about 2.4 ms between the peak values which was accounted for in the curve $p_{gauge,+t}$ to facilitate the comparison. The earlier pressure increase for the gauge particle pressure is caused by the nature of this evaluation method where the gauge detects regular particles before the contact surface registers a contact force (depending on the contact thickness). Nevertheless, this time shift may be neglected for the considered application. Peak pressure values differ about 16 %. However, post-peak mean pressure values are approximately two times higher in the pressure time history evaluated using the contact normal force method.

Within the SMAES project, numerical results will be compared to experimental ones allowing for validation of the novel pressure assessment method using gauge particles.

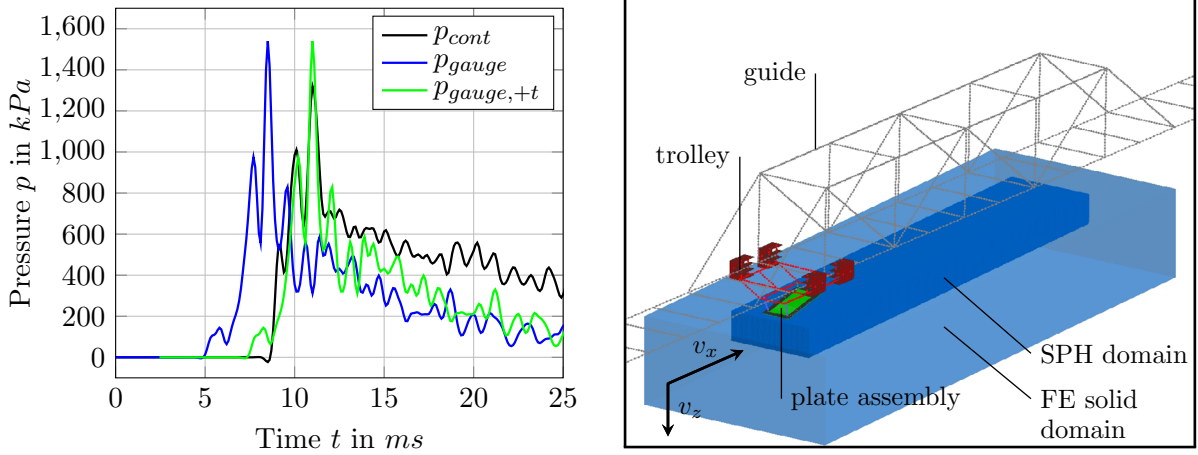


Figure 6: Comparison of pressure time histories between two pressure evaluations methods as shown in figure 3: Pressure via contact normal force over contact area (p_{cont}) and pressure gauge particles (p_{gauge} , $p_{gauge,+t}$), and 3D guided ditching simulation model.

5.4 Three-Dimensional NACA2929 J-Body Ditching

The application of pressure gauge particles to the three-dimensional NACA2929 J-body ditching case [21–23] is used to show the capability of the numerical simulation to model hydrodynamic effects, namely overpressure and suction (negative relative pressure).

The numerical model is symmetrical about the vertical mid plane of the fuselage. Initial velocities are $v_x = 18.28\text{ m/s}$ in horizontal and $v_z = 0.81\text{ m/s}$ in vertical direction. The fuselage is 1.18 m long, weighs 2.83 kg , and has an initial pitch angle of 10° . The water domain is filled with particles with smoothing length $h = 25\text{ mm}$. The model uses a contact separation stress feature [4] as well as a two-phase material model [22] to account for the above mentioned hydrodynamic phenomena.

Figure 7 shows characteristic pressure time distributions at two distinct positions along the center line where overpressure (P_2) and suction (P_5) may be observed. Additionally, contour plots on the right hand side of figure 7 highlight the influence of these hydrodynamic phenomena on the global kinematics in terms of fuselage pitch angle α . During the entire simulation up to $t = 1000 \text{ ms}$, the pitch angle varies between -3° and 33° which agrees well with experimental results in [21].

It is advised that numerical models include capabilities to allow for hydrodynamic phenomena like overpressure, suction and cavitation (necessitates multi-phase fluid models).

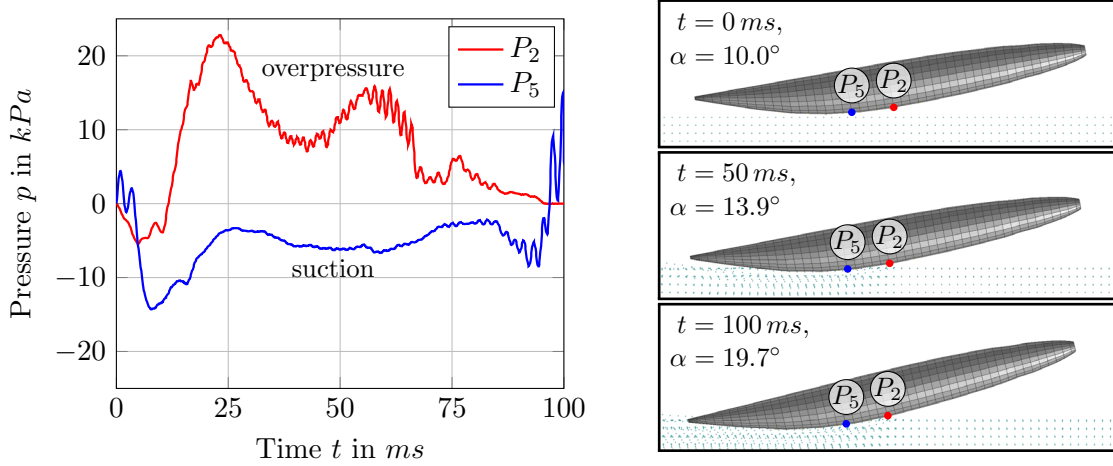


Figure 7: Pressure distributions at two distinct positions (P_2 and P_5) observing overpressure and suction together with contour plots highlighting the effect on global kinematics (pitch angle α).

6 CONCLUSION AND OUTLOOK

In this work fluid-structure interaction models for aircraft ditching analysis have been presented. Furthermore, the necessity of correct and reliable pressure assessment was highlighted as this is seen as a key issue to be solved prior to exploring involved hydrodynamic phenomena. A novel SPH-based pressure evaluation method using gauge particles was presented and demonstrated to give reasonable results. The influences of gauge size ratio, filtering, and two pressure correction methods on pressure results were studied. In general, pressure results could be improved but oscillations and numerical noise remain which may be related to the very short duration of the studied phenomena in combination with the finite size of the particles. Further improvements are expected from introduction of particle regularization methods [23]. The gauge particle method will be applicable to a wide range of other SPH-FE simulations of fluid-structure interaction, e. g. slamming or sloshing. Additionally, pressures assessed by integrating the contact normal force over contact area were compared to gauge particle pressures with the result that peak pressure values were captured well but post-peak mean pressure values were considerably lower for the gauge particle method.

One drawback of this study is the lack of experimental data. Test cases were taken exclusively from literature, hence allowing only for initial validation. NACA pressure results also seem to lack accuracy as compared to today's typical experimental equipment. The pressure sensors used by the NACA in 1951 were rather large which may have resulted in averaging of local pressure peaks. Moreover, the sampling rate of the acquisition system may have been too large to capture peak pressures.

Full validation of the novel pressure assessment method using gauge particles is intended using results of guided ditching tests carried out within the SMAES project (see section 5.3). There the effects of hydrodynamic phenomena and structural flexibility are—for the first time—investigated in an experimental campaign of guided ditching tests. These tests are unique due to the initial conditions and the representative test specimen size, which correspond to full-scale aircraft ditching parameters.

Future work will focus on the influence of impact velocity on pressure results assessed with pressure gauge particles. After full validation of this pressure evaluation method, hydrodynamic phenomena and hydroelasticity under typical ditching loads could be studied. In addition, pressure gauges could be applied to full aircraft ditching simulations to assess the spacial pressure distribution along the bottom fuselage during ditching to enable detailed investigations of interference of hydrodynamic phenomena and global aircraft kinematics.

ACKNOWLEDGMENT

Most of the work leading to the results presented in this paper has received funding from the European Commission's Seventh Framework Programme under grant agreement n° FP7—266172 and was performed within the project “SMAES – SMart Aircraft in Emergency Situations”.

REFERENCES

- [1] Smiley, R. F. *An experimental study of water-pressure distributions during landings and planing of a heavily loaded rectangular flat-plate model*. NACA Technical Note 2453, Langley Field, Virginia, USA, (1951).
- [2] Battley, M.; Allen, T.; Schierlink, J.; Lake, S. and Pherson, P. *Hydroelastic Behaviour of Slam Loaded Composite Hull Panels*. 3rd High Performance Yacht Design Conference, Auckland, New Zealand, (2008).
- [3] Toso, N. *Contribution to the Modelling and Simulation of Aircraft Structures Impacting on Water*. Dissertation, University Stuttgart, Germany, (2009).
- [4] Benítez Montañés, L.; Climent Máñez, H.; Siemann, M. and Kohlgrüber, D. *Ditching Numerical Simulations: Recent Steps in Industrial Applications*. Aerospace Structural Impact Dynamics International Conference, Wichita, Kansas, USA, (2012).

- [5] Climent, H.; Benítez, L.; Rosich, F.; Rueda, F. and Pentecôte, N. *Aircraft Ditching Numerical Simulation*. 25th International Congress of the Aeronautical Sciences (ICAS), Hamburg, Germany, (2006).
- [6] Lindenau, O.; Busch, C.; Streckwall, H.; Bensch, L. and Rung, T. *Validation of a transport aircraft ditching simulation tool*. 6th International KRASH Users' Seminar (IKUS6), Stuttgart, Germany, (2009).
- [7] Macià, F.; Souto-Iglesias, A.; Antuono, M. and Colagrossi, A. *Benefits of using a Wendland kernel for free-surface flows*. 6th SPHERIC Workshop, Hamburg, Germany, (2011).
- [8] Monaghan, J. J. *Smoothed Particle Hydrodynamics*. Annu. Rev. Astron. Astrophys. **30**: 543–574, (1992).
- [9] Monaghan, J. J. *Simulating Free Surface Flows with SPH*. Journal of Comp. Phys. **110**: 399–406, (1994).
- [10] Monaghan, J. J. *Smoothed Particle Hydrodynamics*. Rep. Prog. Phys. **68**: 1703–1759, (2005).
- [11] Aquelet, N. and Souli, M. *Damping Effects in Fluid-Structure Interaction: Application to Slamming Problem*. 7th Int. Symp. on Emerging Technology in Fluids, Structures, and Fluid-Structure Interactions: 233–242, Cleveland, Ohio, USA, (2003).
- [12] Groenenboom, P. *A unified view of SPH wall boundary conditions and particle motion correction methods*. 6th SPHERIC Workshop, Hamburg, Germany, (2011).
- [13] Shepard, D. *A two-dimensional interpolation function for irregularly-spaced data*. 23rd ACM Nat. Conf.: pp. 517—524. New York, New York, USA, (1968).
- [14] Colagrossi, A. *A Meshless Lagrangian Method for Free-Surface and Interface Flows with Fragmentation*. Dissertation, University of Rome La Sapienza, Italy, (2003).
- [15] Parshikov, A. N.; Medin, S. A.; Loukashenko, I. I. and Milekhin, V. A. *Improvements in SPH method by means of interparticle contact algorithm and analysis of perforation tests at moderate projectile velocities*. Int. Journal of Imp. Eng. **24**: pp. 779—796, (2000).
- [16] Parshikov, A. N. and Medin, S. A. *Smoothed Particle Hydrodynamics Using Interparticle Contact Algorithms*. Journal of Comp. Phys. **180**: pp. 358–382 (2002).
- [17] Cha, S.-H. and Whitworth, A. P. *Implementations and tests of Godunov-particle hydrodynamics*, Mon. Not. R. Astro. Soc. **340**: pp. 73–90, (2003).

- [18] Iafrati, A. and Calcagni, D. *Numerical and experimental studies of plate ditching*. 28th Int. Workshop on Water Waves and Floating Bodies, L'Isle sur la Sorgue, France, (2013).
- [19] Campbell, J. *Prediction of aircraft structural response during ditching: An overview of the SMAES project*. Aerospace Structural Impact Dynamics International Conference, Wichita, Kansas, USA, (2012).
- [20] SMAES Consortium *Description of work*. Grant agreement n°266172, Annex I, Seventh Framework Programme, (2010).
- [21] McBride, E. E. and Fisher, L. J. *Experimental investigation of the effect of rear-fuselage shape on ditching behavior*. NACA Technical Note 2929. Langley Field, Virginia, USA, (1953).
- [22] Groenenboom, P. *SPH for two-phase fluid flow including cavitation*. 7th SPHERIC Workshop, Prato, Italy, (2012).
- [23] Groenenboom, P. H. L. and Cartwright, B. K. *Pressure-corrected SPH with innovative particle regularization algorithms and non-uniform, initial particle distributions*. 8th SPHERIC Workshop, Trondheim, Norway, (2013).